

# **Dilution Strategies for Load and NOx Management in a Hydrogen Fuelled Direct Injection Engine**

**Callan Bleechmore and Simon Brewster**  
Orbital Corporation Ltd.

The Engineering Meetings Board has approved this paper for publication. It has successfully completed SAE's peer review process under the supervision of the session organizer. This process requires a minimum of three (3) reviews by industry experts.

All rights reserved. No part of this publication may be reproduced, stored in a retrieval system, or transmitted, in any form or by any means, electronic, mechanical, photocopying, recording, or otherwise, without the prior written permission of SAE.

For permission and licensing requests contact:

SAE Permissions  
400 Commonwealth Drive  
Warrendale, PA 15096-0001-USA  
Email: [permissions@sae.org](mailto:permissions@sae.org)  
Tel: 724-772-4028  
Fax: 724-776-3036



For multiple print copies contact:

SAE Customer Service  
Tel: 877-606-7323 (inside USA and Canada)  
Tel: 724-776-4970 (outside USA)  
Fax: 724-776-0790  
Email: [CustomerService@sae.org](mailto:CustomerService@sae.org)

**ISSN 0148-7191**

**Copyright © 2007 SAE International**

Positions and opinions advanced in this paper are those of the author(s) and not necessarily those of SAE. The author is solely responsible for the content of the paper. A process is available by which discussions will be printed with the paper if it is published in SAE Transactions.

Persons wishing to submit papers to be considered for presentation or publication by SAE should send the manuscript or a 300 word abstract to Secretary, Engineering Meetings Board, SAE.

**Printed in USA**

# Dilution Strategies for Load and NO<sub>x</sub> Management in a Hydrogen Fuelled Direct Injection Engine

Callan Bleechmore and Simon Brewster

Orbital Corporation Ltd.

Copyright © 2007 SAE International

## ABSTRACT

A study has been undertaken on a boosted single cylinder research engine with direct injection of hydrogen. In order to reduce NO<sub>x</sub> emissions and tendency to knock, efforts have been made to reduce the temperatures and rate of heat release during combustion. Lean boosted operation, stoichiometric operation with exhaust gas recirculation, and water injection using a dual fluid direct injector were investigated and NO<sub>x</sub> emissions, thermal efficiency, and combustion stability were compared. Conclusions are developed for specific power optimisation and NO<sub>x</sub> management which may be applied for hydrogen fuelling of small general purpose through to heavy duty engines.

## INTRODUCTION

Hydrogen fuelled internal combustion engines may be regarded as an important step on the way to the hydrogen economy. They offer potentially zero greenhouse gas emissions from a renewable energy source [1].

The current hydrogen infrastructure issue may be addressed through fuel flexibility offered by the internal combustion engine, for example bi-fuel usage with gasoline [2] or CNG and potential for the development of other incremental technologies such as hydrogen CNG mixtures [3] and hydrogen rich gases [4]. Hydrogen ICE's may also offer advantages for cost, durability, climatic capability and fuel purity requirements. Indicated thermal efficiencies of hydrogen fuelled ICE's may exceed 50% [5].

The combustion characteristics of hydrogen make it well suited for internal combustion engines. The wide flammability limits of hydrogen mixtures permit very lean operation [5]. High efficiency from near constant volume combustion is possible due to the high flame speeds of near stoichiometric mixtures. These characteristics however introduce the particular challenges of NO<sub>x</sub> emission control, excess combustion rate and pre-ignition during high load operation, which may limit the specific power output of hydrogen fuelled engines [6].

Manifold delivery of hydrogen presents an immediate route for conversion of existing production engines. Specific power is limited by the displacement of intake air and whilst boosting may offset some of this loss, output may be ultimately limited by premature combustion of the charge at equivalence ratios approaching unity. Direct injection of hydrogen offers an improvement of 42% in volumetric efficiency, and may also enable high load operation at or close to stoichiometry [7].

In this study engine data are generated from an hydrogen fuelled direct injected and boosted engine. In particular several dilution strategies are investigated that may enable optimisation of specific output and control of NO<sub>x</sub> emissions.

## EMISSION REGULATIONS

The exhaust gases of internal combustion engines are typically regulated for cleanliness. Standards are defined through respective emission regulations for engine application, geographical region, test cycle and pollutant. Test cycles may be defined according to engine or vehicle operation, and may include transient and high load conditions. Regulated pollutants typically include hydrocarbons, carbon monoxide, oxides of nitrogen, particulate matter and potentially carbon dioxide. In this regard oxides of nitrogen are the only pollutant of concern from hydrogen fuelled internal combustion engines, and as NO<sub>x</sub> mitigation strategies are load dependent the test cycle is also highly pertinent to achieving emission compliance.

Table 1 presents a brief overview of emission regulations according to engine application with specific reference to NO<sub>x</sub> thresholds, and identifies whether a test cycle includes higher load operation. The regulations shown will typically apply in the 2010 timeframe, and for brevity include selected standards that indicate the overall challenge for hydrogen fuelled ICE's. It may be observed that for all engine classes a restriction applies for emissions of NO<sub>x</sub>, and in general this restriction applies to higher and full load operation. It is therefore clear that hydrogen fuelled ICE's with any associated aftertreatment must typically deliver low emissions of NO<sub>x</sub> across the engine load range.

Engine Class	Sub Class	Standard	NOx Level	Test Description
General Purpose	80cc <displacement <225 cc	CARB Phase 3	10* g/kWh	part and full load *NOx + HC
	displacement > 225 cc		8* g/kWh	
Marine		CARB 4 Star	5* g/kWh	
Motorcycle	2 wheels	Euro 3	0.150 g/km	part load only
	3 & 4 wheels		0.25 g/km	
Light Duty Vehicles	up to 14 passengers	SULEV2	0.02 g/mi	part and high load
	all passenger and LD <3500 kg GVW	Euro 5	0.06 g/km	part load only
	3501 - 12000 kg GVW		0.082 g/km	
Heavy Duty Vehicles	8501 - 14000 lbs GVW	ULEV	0.2 g/bhp.h	part and full load
		SULEV	0.1 g/bhp.h	
	>14000 lbs GVW	ULEV	0.2 g/bhp.h	
		Euro 5	2.0 g/kWh	

**Table 1 Summary of NOx emission regulations.**

## LITERATURE REVIEW

Research and development of hydrogen fuelled IC engines has expanded during the last decade as pressures for cleaner and renewable propulsion systems increase. The key challenges are related to the high load operation required to match the power density of current gasoline fuelled engines.

Certain properties of hydrogen are advantageous over other fuels whilst other properties present challenges. A comparison is presented in Table 2.

Property	Hydrogen	Methane	Gasoline
Limits of flammability in air (vol %)	4-75	3.5-15	1-7.6
Laminar burning velocity in air (m/s)	2-2.3	0.37-0.43	0.37-0.43
Min energy for ignition in air (mJ)	0.02	0.29	0.24
Auto-ignition temperature (K)	858	813	501-744
Quenching gap in air (mm)	0.64	2.03	2
Diffusion coefficient in air (cm <sup>2</sup> /s)	0.61	0.16	0.05
Density (kg/m <sup>3</sup> )	0.0838	0.7174	700-750
Flame temperature in air (K)	2318	2148	2470
Lower heating value (MJ/kg)	120	50	44
Research Octane Number	>130	>120	90-100
Normal Boiling Point (K)	20.3	111.6	310-478
Stoichiometric air fuel ratio (:1)	34.3	17.23	14.6

**Table 2 Fuel properties [8]**

Stoichiometric mixtures of hydrogen and air have 18% lower calorific value than gasoline stoichiometric mixtures [7] resulting in a significant power deficit in engines with external mixture formation. The reduction of peak power can be up to 50% [9] as abnormal combustion, such as pre-ignition and back-fire limit air fuel ratio. Compared to engines with direct injection, external mixture aspirating engines have returned higher efficiencies, permit extended lean operation, lower cyclic

variations and lower NOx production at part load due to better mixture homogeneity and reduced pumping work.

Direct injection has been demonstrated to overcome some of the short falls of engines with external mixture formation. The calorific value of stoichiometric mixture is 17% higher than that of gasoline mixtures [7]. Loads of up to 1500 kPa IMEP have been achieved with a naturally aspirated DI engine [6].

Abnormal combustion in the form of back-fire, pre-ignition, and knock has been reported during high load operation of both internal and external mixture formation hydrogen fuelled engines.

Backfire can be reduced in PFI engines by delaying the injection event such that the end of injection occurs just prior to intake valve closure [10]. This allows for the residual gases to be cooled by the fresh charge prior to the injection event. A very rich, non-ignitable mixture enters the cylinder, meaning that a combustible mixture does not exist outside of the cylinder.

The wide flammability limits of hydrogen make it susceptible to pre-ignition. Pre-ignition is the chief cause of limited torque in the hydrogen fuelled engine [5]. The source of the uncontrolled ignition seems to be dependent on the operating condition but is not yet fully understood.

Knock like combustion is another abnormality observed during high load operation. There is evidence that hydrogen knock is caused by excessive flame speeds rather than an end gas reaction [11]. The effective octane number for hydrogen is dependent on the equivalence ratio of the mixture. Since the knocking phenomenon in hydrogen mixtures differs from gasoline knock, it could be argued that octane rating is an inappropriate measure of hydrogen's tendency to knock.

NOx is the only significant pollutant from hydrogen fuelled IC engines, and imposes limits on medium to high load operation. Various operating strategies have been developed to reduce NOx emissions. Operation

with equivalence ratios less than 0.5 can return engine out NO<sub>x</sub> concentrations of less than 100ppm [8]. For leaner mixtures, NO<sub>x</sub> emissions are close to zero [10], however intake manifold boosting is required to recover the power losses from lean operation.

Exhaust gas recirculation (EGR) is another strategy indicated to reduce NO<sub>x</sub> emissions. The exhaust gases, which consist largely of water and nitrogen gas increase the specific heat capacity of the induced charge, reducing combustion rates and temperatures. An advantage of using EGR and stoichiometric mixtures over the lean burn strategy is the ability to use a standard three way catalyst to further reduce NO<sub>x</sub> emissions.

The effectiveness of a diluent on reducing engine out NO<sub>x</sub> emissions has been shown to be directly proportional to the diluents' specific heat capacity [12].

Recent studies comparing the effectiveness of lean burn and EGR at controlling NO<sub>x</sub> have shown that EGR performs better for similar power outputs [13]. The same study showed that the effectiveness of EGR on reducing NO<sub>x</sub> is unaffected by the temperature of the recirculated gases.

Water injection has been used previously to suppress pre-ignition in port fuelled hydrogen fuelled engines, although the effects on NO<sub>x</sub> production were not documented [14].

A study into the effect of fuel humidity was conducted to test the viability of storage of hydrogen in an aqueous solution of sodium borohydride. Steam was introduced into the air fuel mixture externally and NO<sub>x</sub> emissions, ISFC and combustion stability was compared at lambda values of 1.0, 1.5 and 2.0. An 83% decrease in NO<sub>x</sub> concentration was reported at stoichiometric operation with minor degradation of combustion stability [14].

## TEST SETUP

### ENGINE TEST BED

Research has been carried out with a 4-stroke single cylinder spark ignition research engine. The engine has a centrally located direct injector with hydrogen supply at 2000 kPa, see Figure 1. In-cylinder pressure was measured using a water-cooled piezoelectric type pressure transducer (Type KISTLER 6051). The engine specifications are detailed in Table 3.

Equivalence ratio was determined from both exhaust gas analysis and mass flow measurement of air and fuel. Mass flow of air was measured using a laminar flow element with differential pressure cell, and mass flow of fuel with a Coriolis mass flow meter. For indication a wide band exhaust gas oxygen sensor was also fitted.

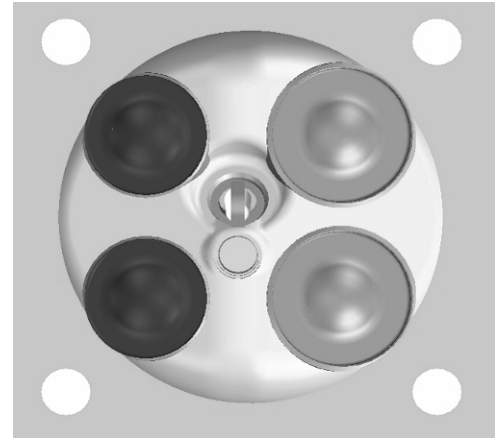


**Figure 1 Four valve head with centrally located injector and spark plug**

Engine	Single cylinder
Displacement	454 cc
Bore	82 mm
Stroke	86 mm
Number of valves	4
Compression ratio	10.7:1
Engine speed	2000 RPM
Piston	Flat top
EVO	133 °aTDC <sub>f</sub> (587 °bTDC <sub>f</sub> )
EVC	357 °aTDC <sub>f</sub> (363 °bTDC <sub>f</sub> )
IVO	364 °aTDC <sub>f</sub> (356 °bTDC <sub>f</sub> )
IVC	583 °aTDC <sub>f</sub> (137 °bTDC <sub>f</sub> )
Pressure Charging	Electrically driven supercharger

**Table 3 Engine specification**

The flow of exhaust gas into the intake plenum was controlled via a valve. Water at ambient temperature could be supplied to an exhaust gas heat exchanger to cool the exhaust gases entering the intake plenum to approximately 50 °C.

An electrically driven supercharger was used to accurately control boost pressure independent from engine speed. The exhaust back pressure was adjusted to represent that of a supercharged engine.

### FUEL INJECTOR

A gaseous direct injector (Figure 2) was used for the duration of the tests with a fuel supply pressure of 2000 kPa. The low density of hydrogen, and the reduced time available for injection, requires an injector with a high flow rate, whilst providing accurate metering for low load operation. The prototype injector was originally developed to meet these challenges for boosted CNG engines of 450cc capacity per cylinder [15].

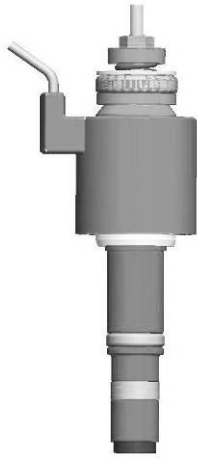


**Figure 2 Gas direct injector [15]**

### WATER INJECTION

A dual fluid injector was used to deliver the hydrogen and a well atomized spray of water directly into the cylinder. Distilled water was supplied at 1000 kPa whilst the hydrogen fuel was supplied at 900 kPa to obtain a 100 kPa differential across the water injector. The operation of the dual fluid injector has been documented in work by Cathcart et al. [16].

The dual fluid direct injector used for the water injection was originally developed for the delivery of well atomised liquid fuel sprays, see Figure 3. The injectors placed in series separate the water metering event from the fuel delivery event, see Figure 4.

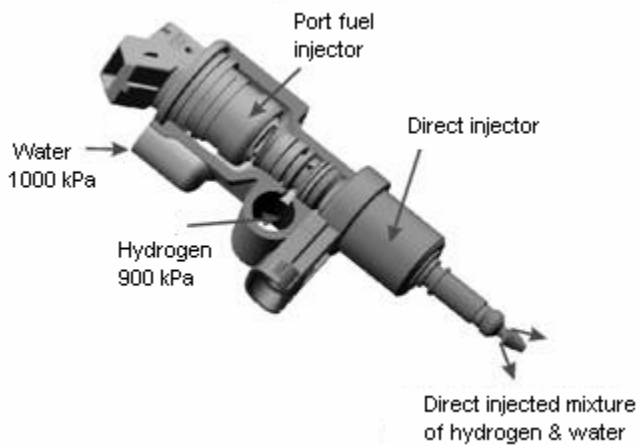


**Figure 3 Dual fluid injector for injection of water and hydrogen fuel.**

The water metering event is separate from the injection event. Since the fuel is in the gaseous phase, the fuel metering and injection event are combined.

### INJECTION SEQUENCING

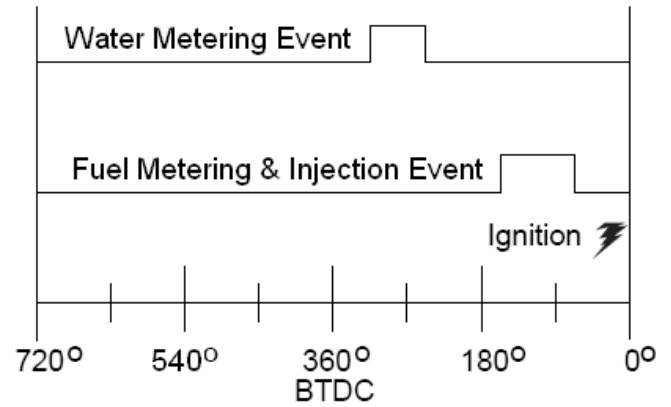


**Figure 4 Water metering and injection event sequence.**

### Spray Visualisation

Images were captured using a LaVision camera. The images were captured and the background image subtracted. The camera has a field of view 40mm high. The amount of air injected per cycle was held constant throughout the spray visualisation tests.

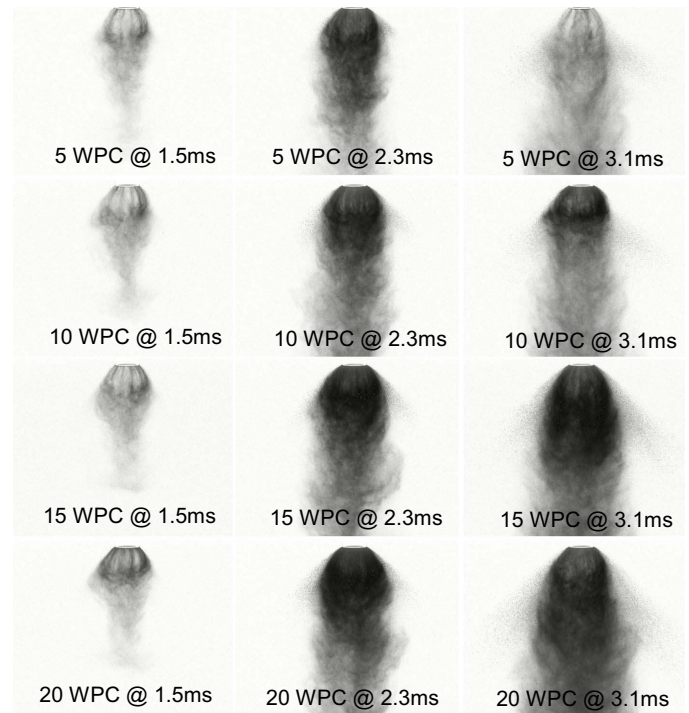


**Figure 5 Spray visualisation for all the water injection amounts used.**

Figure 5 shows the spray formation from the dual fluid injector. The initial spray development is similar for all of the water durations. A dense plume develops 2.3ms after the start of injection and is dispersed into a finer spray.

## Particle size measurement

Particle size measurements were conducted using a Malvern Mastersizer. Measurements were taken 40mm from the tip of the injector at time delays of 0 to 20ms after the start of injection. The results were then weighted against the volume concentration of the spray. The results are summarised in Table 4 below.

Volume Concentration Weighted Results (Trigger times of 0 to 20 ms)	
WPC (mg/injection)	SMD (micron)
5	12.8
10	15.2
15	17.6
20	18.4

**Table 4 Particle size results.**

The Sauter mean diameter is smallest for the 5 WPC injection and increases for the longer water durations. This is due to the greater energy requirement for atomisation of the increased water flux through the injector nozzle.

## TEST PROCEDURE

The testing on the direct injection hydrogen engine can be divided into 4 phases. Initially, sweeps of injection timing, ignition timing, equivalence ratio and load were completed to establish a baseline for efficiency, NOx production and combustion stability. The next phase involved running lean and boosting to increase load. Experiments where EGR was used as a diluent were then undertaken. The injector was changed to a dual fluid type and the effects of water injection into the cylinder were investigated.

## TEST RESULTS

### HYDROGEN DI BASELINE

An initial investigation into the effects of injection timing, equivalence ratio and load was undertaken to gain an understanding of hydrogen combustion in this application. Trends are similar to those in literature and summary data are presented here for reference.

### Injection Timing

Start of injection was swept from 95 to 255 °bTDC in 40° increments. At each injection timing spark advance was varied between -10 and 20 °bTDC with 300 kPa peak IMEP. Early injection timing could not be maintained at medium to high loads due to the onset of excessive backfire. By setting the start of injection (SOI) to 135 °bTDC, after IVC, backfire was eliminated. For consistency, data presented at 300 kPa IMEP elsewhere in this paper utilise an SOI of 135 °bTDC.

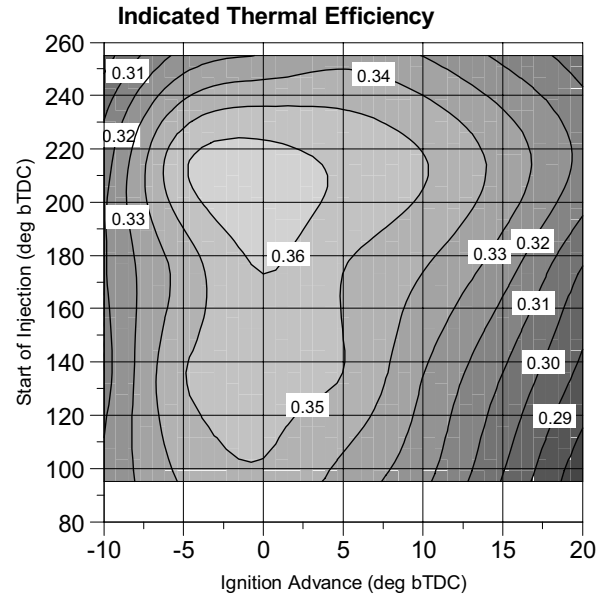


**Figure 6 Indicated thermal efficiency at 300 kPa IMEP and  $\phi=0.5$ .**

At optimal or retarded ignition advance (Figure 6) SOI later than 220 °bTDC has a small effect on efficiency. At advanced ignition timings retarded SOI excessively promotes burn rate and overly advances combustion phasing which reduces efficiency.

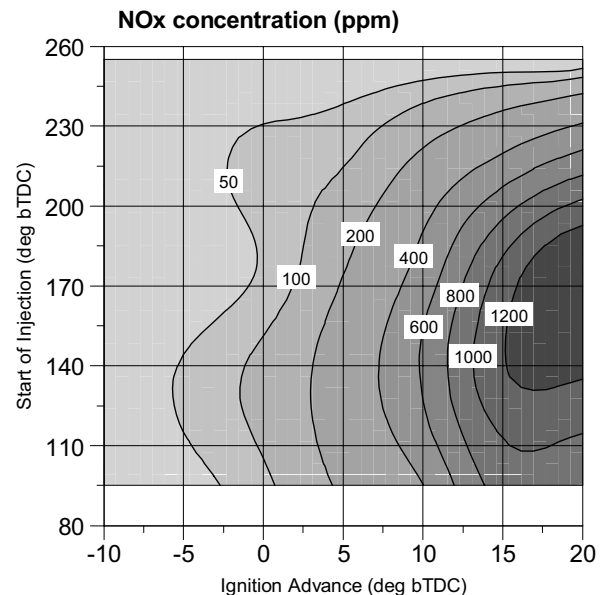


**Figure 7 NOx concentration at 300 kPa IMEP and  $\phi=0.5$ .**

When the ignition timing is optimised to maximise IMEP, NOx concentration is somewhat independent of SOI (Figure 7). At overly advanced ignition timings, NOx concentration is determined by the increased flame temperature arising primarily from higher peak cylinder pressures.

## Equivalence Ratio

Equivalence ratio was varied from the lean stability limit to the onset of excess burn rate and hydrogen type knock at a range of loads. Data at loads of 300 and 900 kPa IMEP are presented here to illustrate typical trends. The start of injection for the following tests is 135° bTDC.

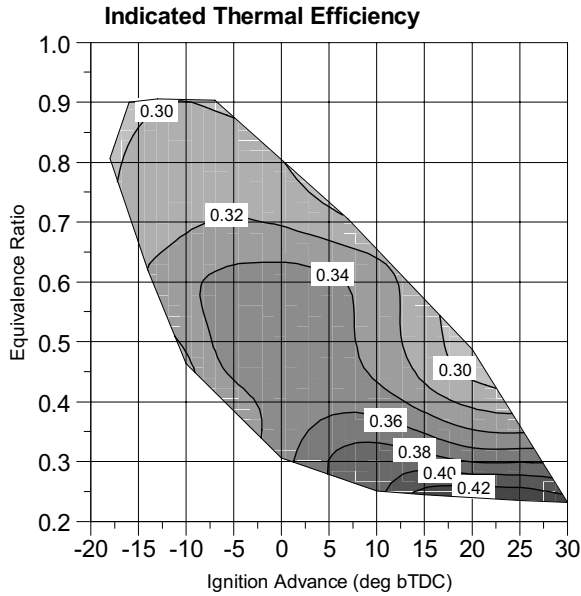


**Figure 8 Indicated thermal efficiency at 300 kPa IMEP.**

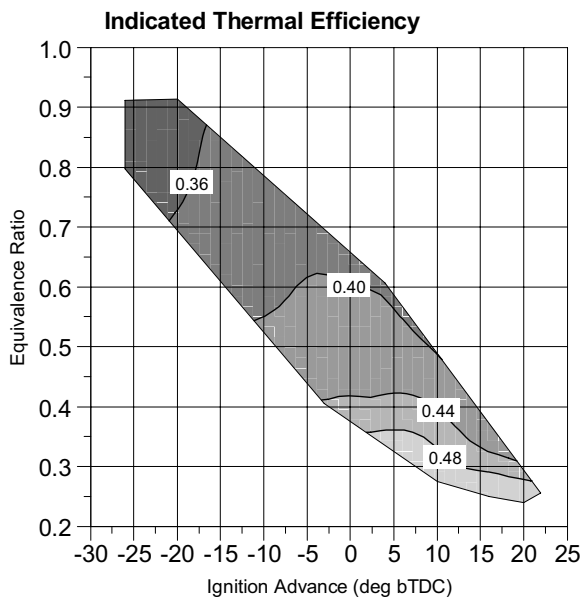


**Figure 9 Indicated thermal efficiency at 900 kPa IMEP.**

Decrease in equivalence ratio yields increased thermal efficiency (Figures 8 & 9), due predominantly to reduction of pumping work and lower heat losses at higher dilution. The reduction of pumping work comes from opening the throttle with constant fuel delivery rate.

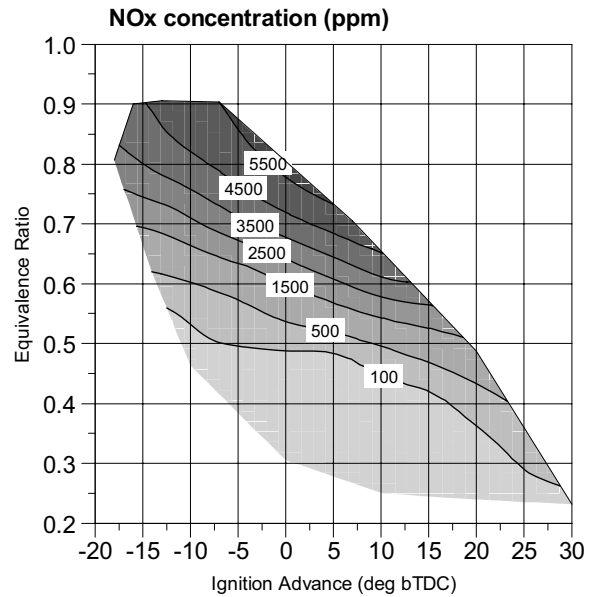


**Figure 10 NOx concentration at 300 kPa IMEP.**

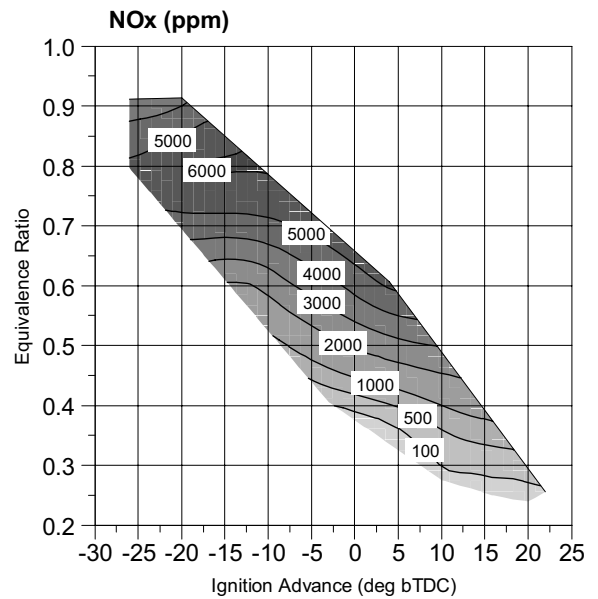


**Figure 11 NOx concentration at 900 kPa IMEP.**

NOx production was observed to increase sharply with increase in equivalence ratio (Figures 10 & 11). At 900 kPa IMEP load, NOx showed a declining trend at equivalence ratios higher than 0.8. The trends are understood in terms of the relative effects of combustion temperature and oxygen concentration which together determine the production of NO [17]. NO formation rate increases with combustion temperature in response to increase in load or equivalence ratio. As equivalence ratio approaches unity the reduction in oxygen concentration reduces the rate of NO formation resulting in a maximum at a lean condition which is load dependent.

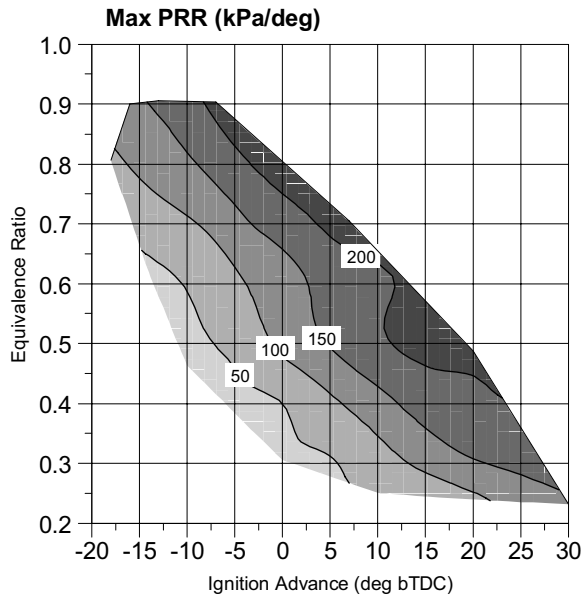


**Figure 12 Maximum cylinder pressure rise rate at 300 kPa IMEP.**

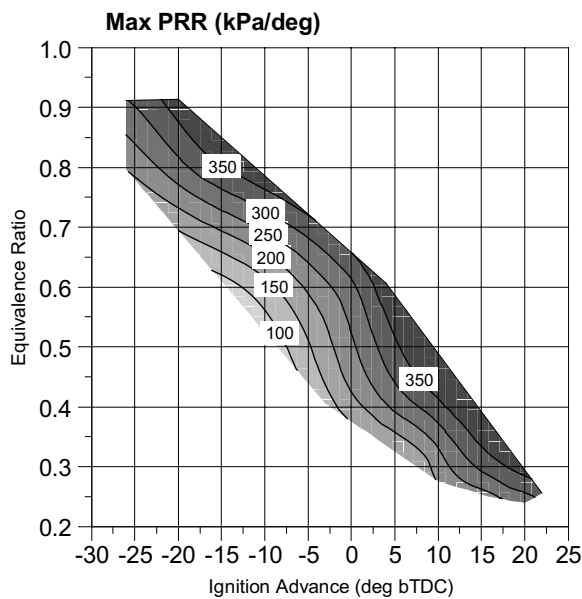


**Figure 13 Maximum cylinder pressure rise rate at 900 kPa IMEP.**

Rate of combustion is indicated in Figures 12 & 13 by maximum pressure rise rate (PRR). The maximum pressure rise rate increases as the equivalence ratio approaches unity, requiring more retarded ignition timing.

Load

Data are presented at a fixed equivalence ratio ( $\phi=0.6$ ) to illustrate the effect of variation in engine load.

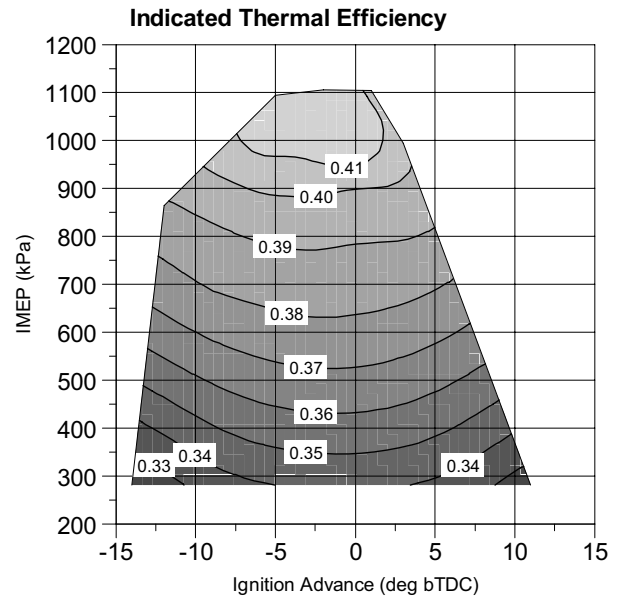


**Figure 14 Indicated thermal efficiency at  $\phi=0.6$ .**

At fixed equivalence ratio ( $\phi=0.6$ ), increased load increases the thermal efficiency (Figure 14) which is primarily attributed to reduced pumping work.

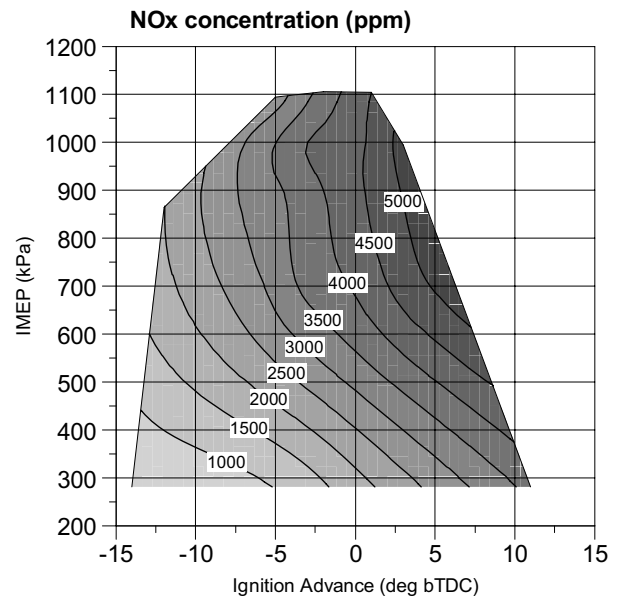


**Figure 15 NOx concentration at  $\phi=0.6$ .**

At a fixed equivalence ratio ( $\phi=0.6$ ), NOx generation (Figure 15) is determined by peak burned gas temperatures, and therefore is a function of load and spark advance.

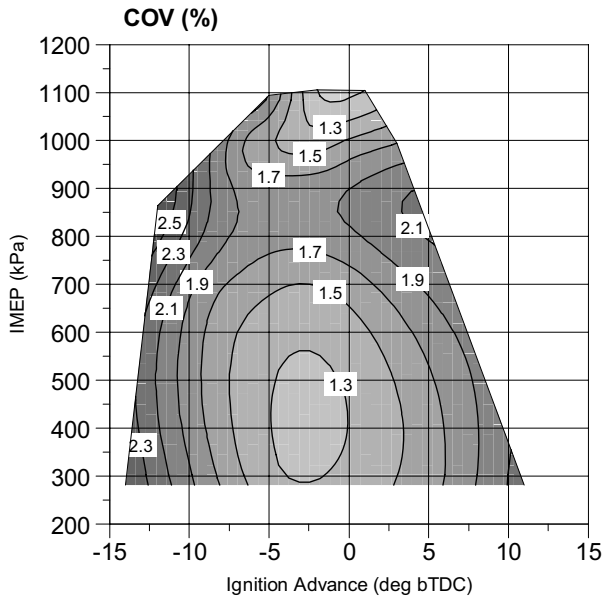


**Figure 16 Combustion stability at  $\phi=0.6$ .**

Combustion stability (Figure 16) is typically observed at low levels and increases at excessively retarded ignition timing.

Overview at Fixed Speed

The following data summarise combustion behaviour in response to variation in load and equivalence ratio. The wide flammability limits of hydrogen could be observed with combustion at  $\phi=0.2$ .

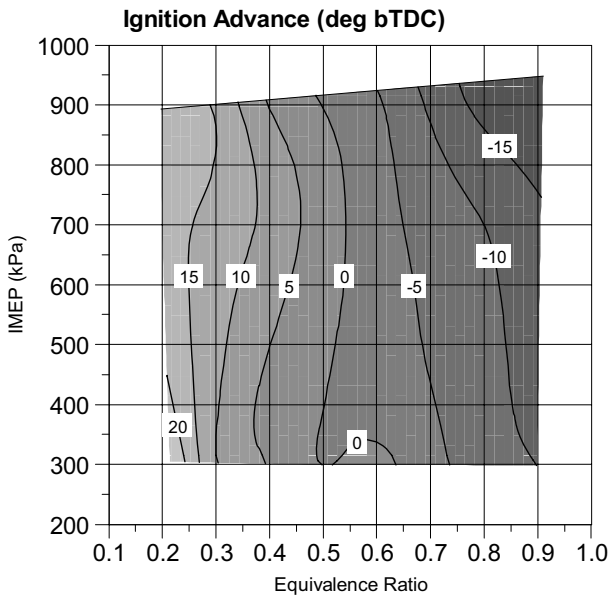


**Figure 17 Optimum or limit ignition timing.**

At lower equivalence ratio optimum ignition timing is basically independent of the load condition (Figure 17). As equivalence ratio approaches unity and load is increased, the burn rate increases and approaches the

limiting condition. In consequence ignition advance is retarded.

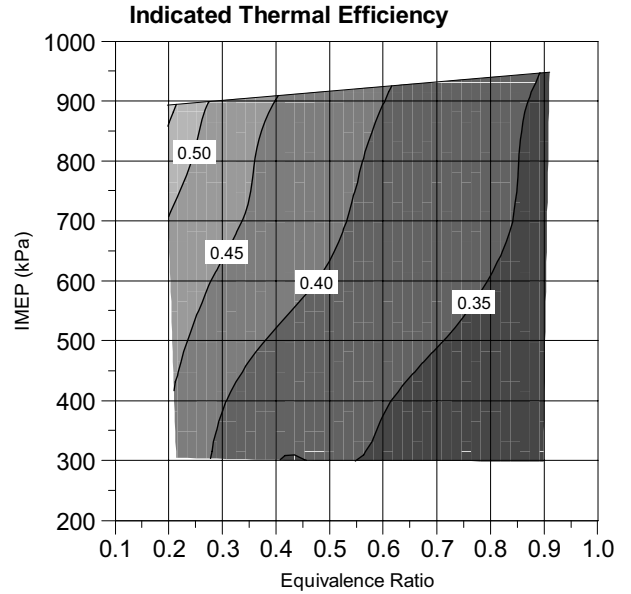


**Figure 18 ITE at optimum or limit ignition timing.**

Indicated thermal efficiency (ITE) increases with increasing load and decreasing equivalence ratio (Figure 18) in response to reduction in pumping work and lower heat loss.

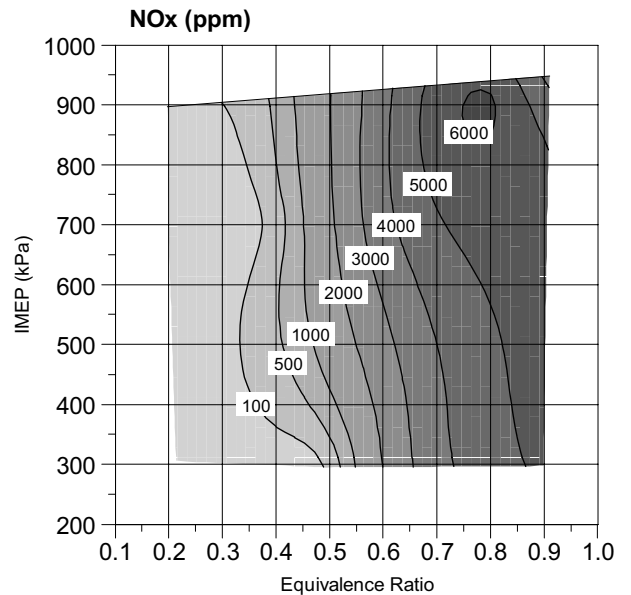


**Figure 19 NOx at optimum or limit ignition timing.**

NOx concentration is primarily dependent on equivalence ratio (Figure 19). High dilution suppresses and may virtually eliminate the formation of NOx emissions at all engine loads.

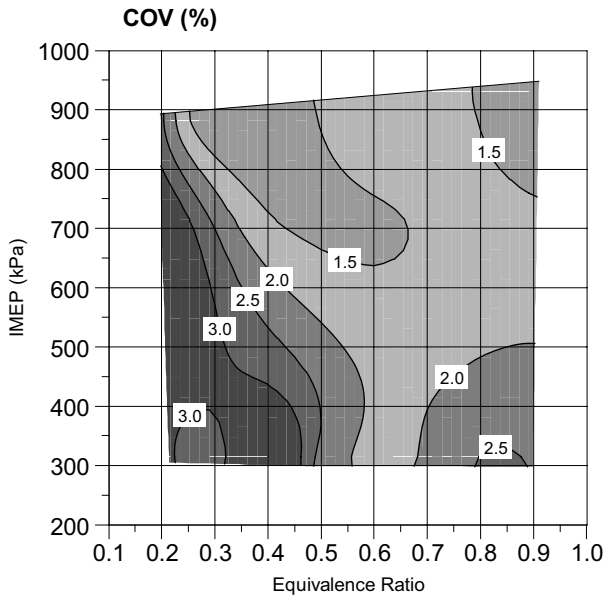


**Figure 20 Combustion stability at optimum or limit ignition timing.**

Combustion stability (Figure 20) is again typically observed at low levels with instability increasing towards the lean operation limit, particularly at lighter loads.

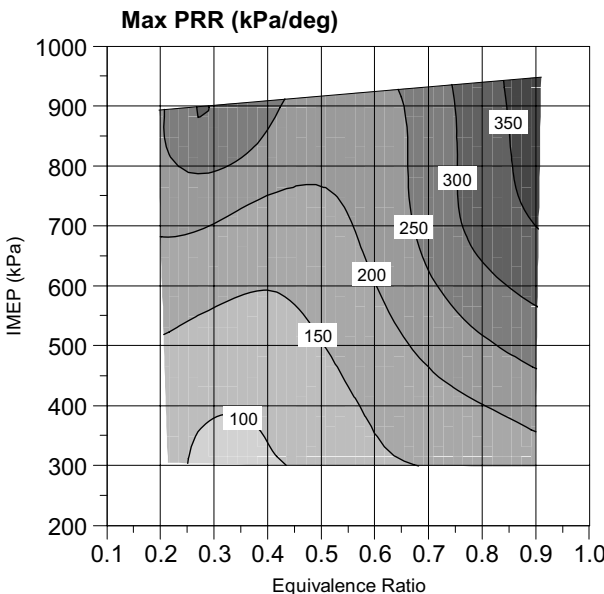


**Figure 21 Maximum pressure rise rate at optimum or limit ignition timing.**

Burn rate, as indicated by maximum pressure rise rate (Figure 21), increases with engine load and rate of increase is substantially influenced by equivalence ratio. At each engine load a certain equivalence ratio yields a minimum burn rate.

#### ABNORMAL COMBUSTION

In addition to combustion instability, certain phenomena are reported below that limit the envelope of engine operation.

#### Backfire

Back-fire is observed as an audible event and abnormal pressure increase in the intake system occurring with intake valve open and with SOI some time before intake valve closure. The mixture self ignites before the intake valve has closed causing a flame to flash back into the intake port. Back-fire was eliminated by injecting only after IVC, although injection immediately prior to IVC was also observed to be effective.

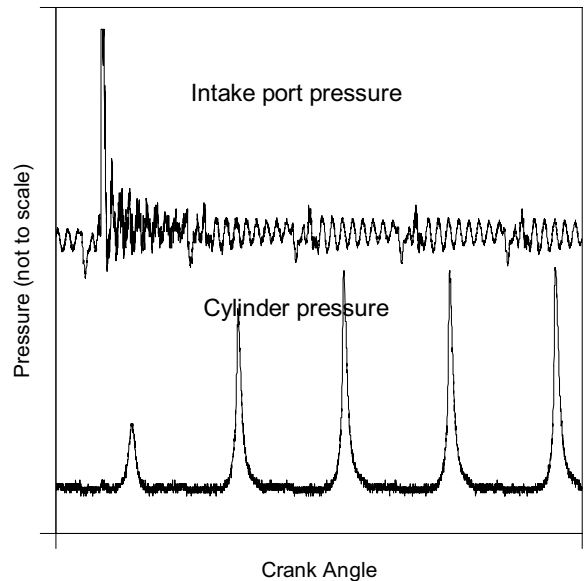


**Figure 22 Early back-fire.**

In this event (Figure 22) back-fire occurs at an early stage with a substantial pressure pulse in the intake port, and misfire results as the charge has combusted before IVC. Combustion pressure in the following cycle is also partially reduced from normal levels due to re-induction of combusted gases. Combustion returns to normal by the third cycle.

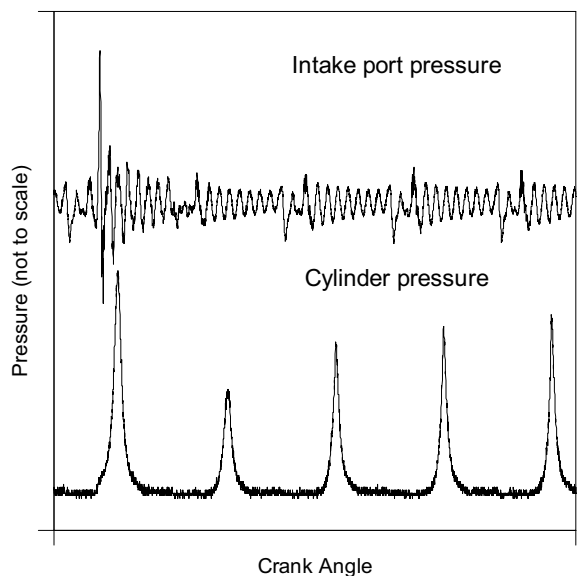


**Figure 23 Late back-fire.**

In this event (Figure 23) back-fire occurs at a later stage with a lower pressure pulse in the intake port. In this instance combustion is only partially complete at time of intake valve closure resulting in early and excessive rise in cylinder pressure. The following cycles are affected as before.

**Knock-like Combustion**

The knock like phenomenon shown in the single cycle in Figure 24 was observed with increasing burn rate at higher load and equivalence ratio approaching 1. The higher effective octane number of hydrogen indicates that auto-ignition of the end gas may not explain this phenomenon. It may be attributed in part to the sustained high burn rate of the main combustion event causing a resonance in the chamber.

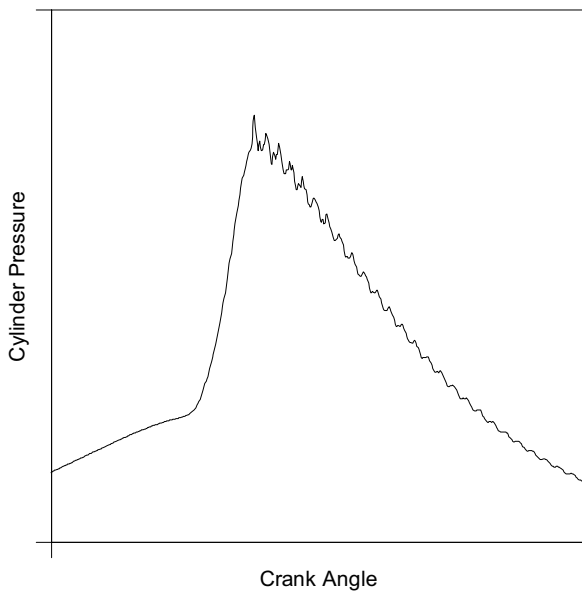


**Figure 24 Knock-like combustion.**

Engine operation at equivalence ratio approaching 1 and the ignition advance achievable at higher loads were limited by this phenomenon, although at moderate levels it was not felt to present a risk of engine damage.

**Pre-ignition**

Pre-ignition as indicated by premature cylinder pressure increase was noted to occur at higher loads and with equivalence ratio close to 1, in association with the highest rates of pressure rise. This presented a high risk of engine damage.

**DILUTION WITH EXCESS AIR**

Tests were completed at 700 kPa IMEP whilst equivalence ratio was varied from 0.2 to 0.8. Equivalence ratios richer than 0.8 were not tested due to the onset of knock-like combustion. Boosting was required to achieve 700 kPa IMEP for equivalence ratios 0.4 and 0.2. The start of injection was set to 135 °bTDC

to prevent backfire into the intake manifold and to allow the maximum time for in-cylinder mixing.

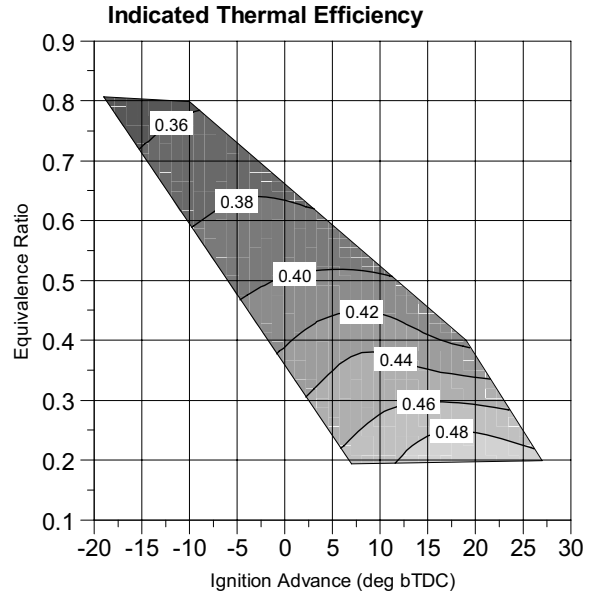


**Figure 25 ITE at 700 kPa IMEP.**

Decrease in equivalence ratio (Figure 25) yields increased indicated thermal efficiency, arising from reduction of pumping work and lower heat losses at higher dilution. Pumping losses decrease as the manifold pressure increased from 80 kPa absolute at  $\phi=0.8$  to 180kPa absolute at  $\phi=0.2$ . Relative brake efficiencies will be moderated according to the selected boosting technology, whilst brake efficiency in this instance is somewhat redundant due to the boosting mechanism used.

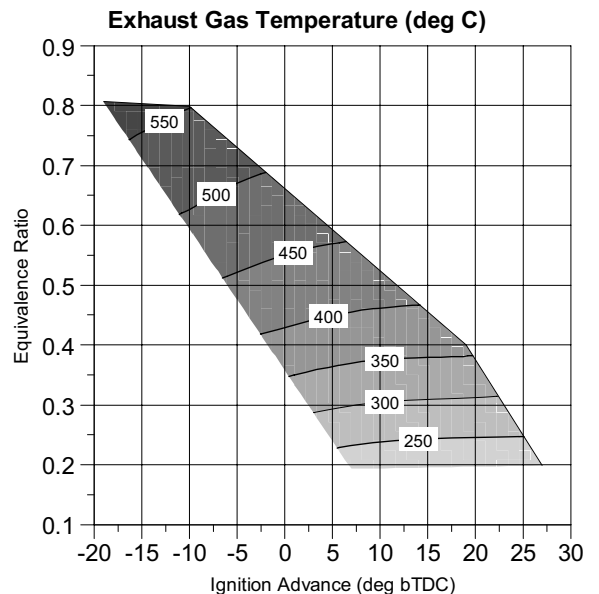


**Figure 26 EGT at 700 kPa IMEP.**

Reduction in combustion temperature and associated heat losses is evident from the response of exhaust gas temperature to increased dilution (Figure 26).

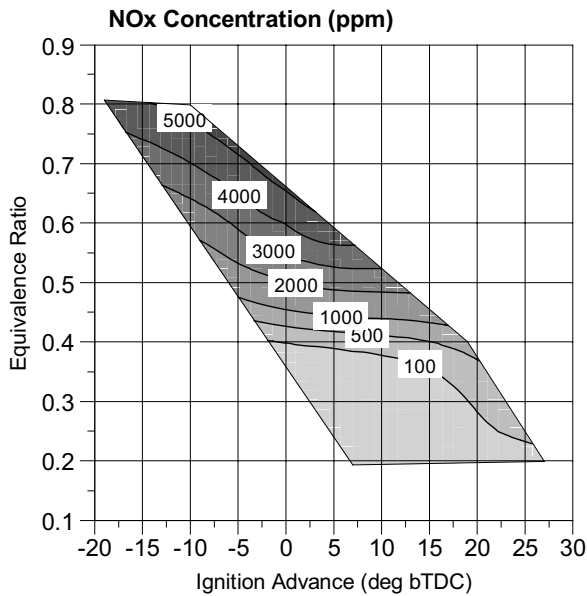


Figure 27 NOx concentration at 700 kPa IMEP.

NOx formation drops from 5000ppm at  $\phi=0.8$  to below 100ppm for  $\phi<0.4$  (Figure 27), arising from reduced flame temperatures at increased dilution.

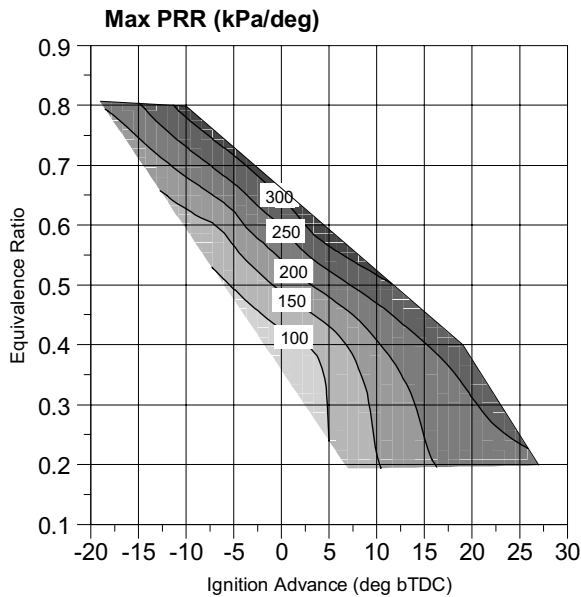


Figure 28 Maximum pressure rise rate at 700 kPa IMEP.

Burn rate reduces as dilution increases (Figure 28), and at high dilution the response of burn rate to ignition advance is substantially moderated.

Combustion stability (Figure 29) decreases as dilution increases due to longer combustion durations and the

approach of lean combustion limits. At  $\phi=0.2$  combustion stability is marginal at the extremes of ignition advance.

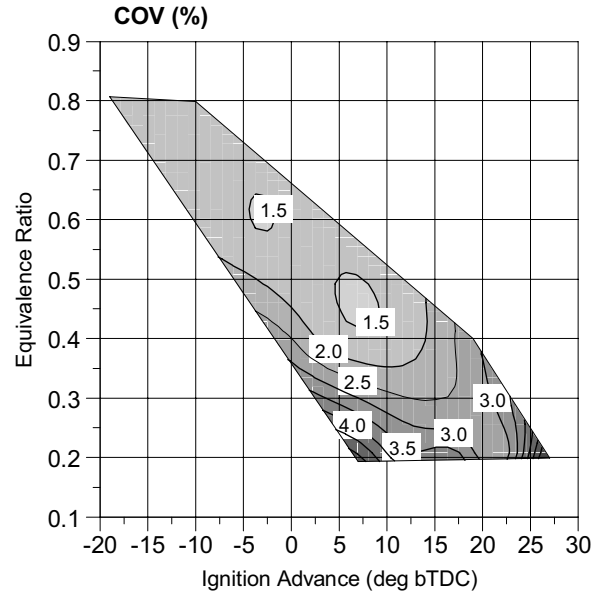


Figure 29 Combustion stability at 700 kPa IMEP.

#### DILUTION WITH EGR

To establish a baseline, a spark sweep was measured at wide open throttle and a lean equivalence ratio. Without altering the fuelling rate and with the EGR valve fully open, fresh air mass flow was reduced by closing the throttle until the stoichiometric condition was reached. Another spark sweep was measured for the hot EGR state. The EGR was then cooled and a spark sweep either side of MBT was measured. Unlike the other tests outlined in this paper, fuelling rate, not load, was held constant.

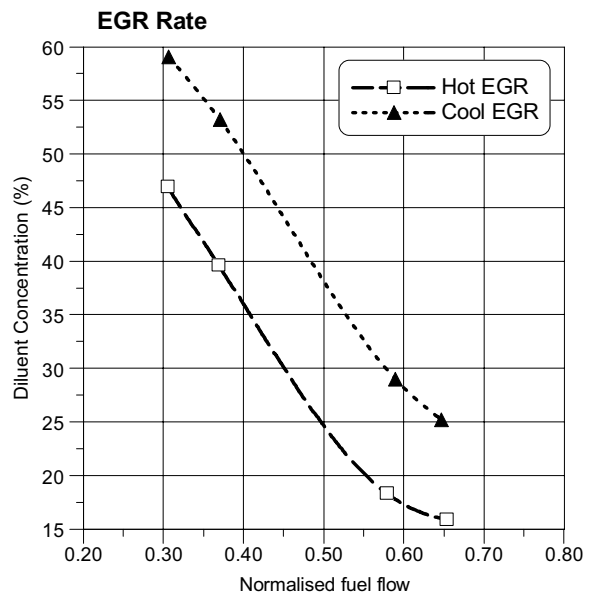


Figure 30 EGR rate.

Rates of EGR expressed in terms of mass are shown in Figure 30. Fuel flow is expressed as a proportion of that required to achieve  $\phi=1$ .

vapour possesses a higher specific heat capacity and will slow combustion more than dilution with excess air.

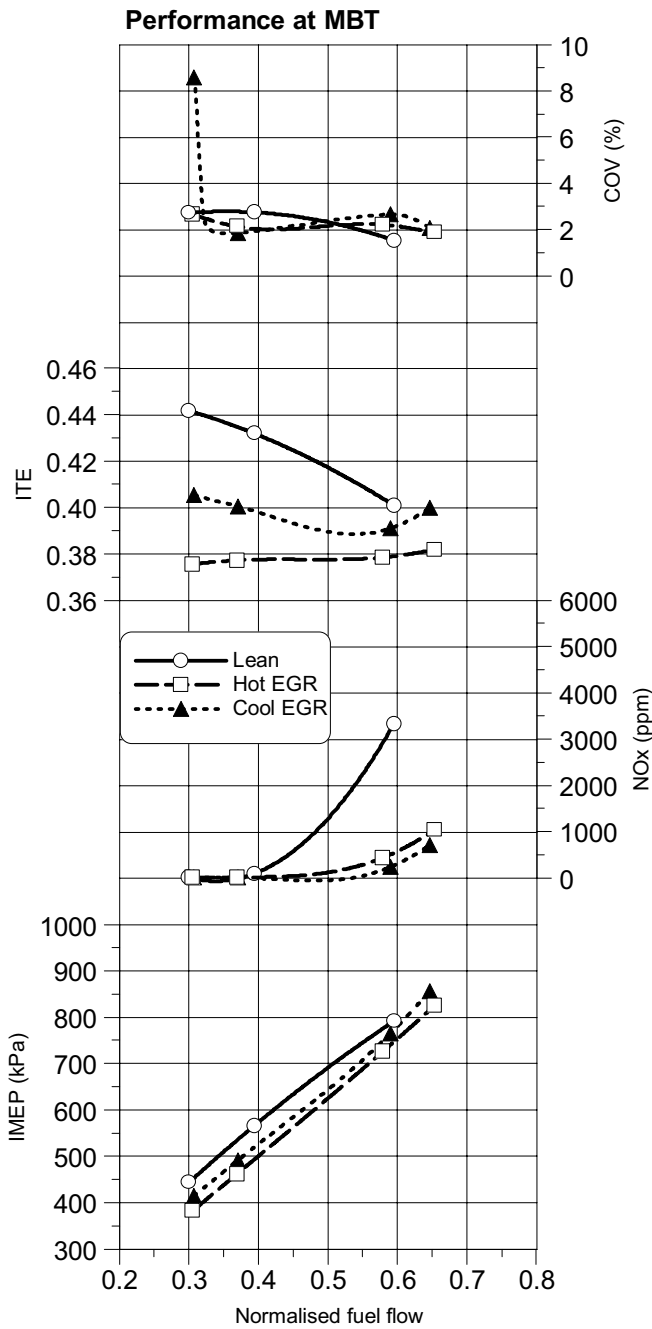


Figure 31 ITE & NOx response to EGR.

As shown in Figure 31, ITE is lower when EGR is used. Cooled EGR yields higher ITE than hot EGR. These trends may be understood in terms of losses to charge temperature and heat losses from the charge.

At the MBT point of each curve, NOx was reduced by 87% when EGR was introduced. The reduction increased to 93% when the EGR was cooled. The decrease in NOx emissions may be attributed to lower peak pressures and temperatures when diluted with EGR. EGR consisting of primarily nitrogen gas and water

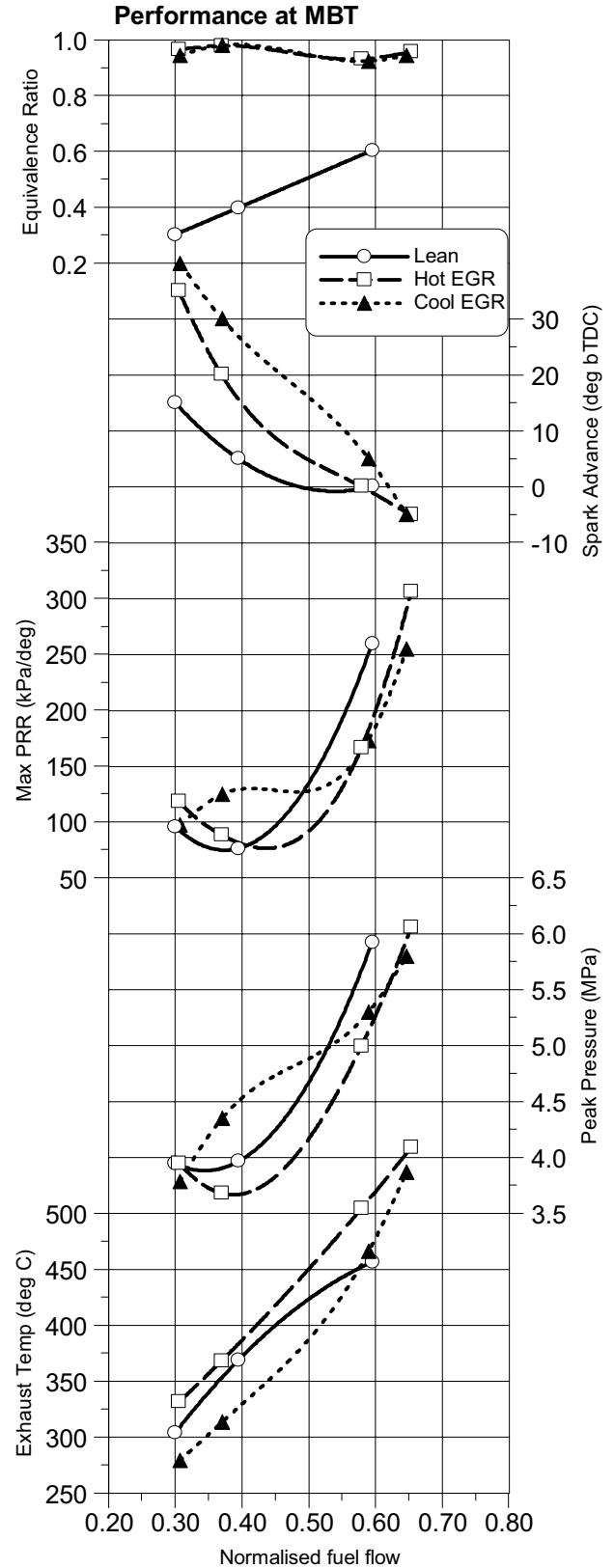


Figure 32 Combustion response to EGR.

Figure 32 shows that combustion stability was optimal at higher load for lean operation, increasing from 1.7% to

2.1% with the introduction of EGR at the MBT point. Cooling the EGR gave a COV rise to 2.6%. At medium load the stability with lower  $\phi$  deteriorates, and at highest dilutions there is evidence that high rates of EGR may cause significant deterioration in stability.

Exhaust temperature is highest for the uncooled EGR due mainly to the elevated inlet temperature. At higher load a reduction in the maximum cylinder pressure rise rate and peak pressure is observed as EGR is introduced.

Operation at  $\phi=0.8$  was not sustained due to the on-set of excessive burn rates. With the introduction of EGR at the same fuelling rate, burn rates are moderated. The introduction of cooled EGR allowed loads of 850 kPa IMEP to be achieved at  $\phi=1$ , showing a potential to extend the naturally aspirated upper load limit.

### DILUTION WITH INJECTION OF WATER

Tests were conducted at 600 kPa IMEP  $\phi=1$ . Load was limited by maximum gas pressure, which was in turn limited by required pressure drop at the water injector and the maximum water pressure that could be sustained by the hardware. The amount of water injected per cycle was varied from 0 to 20 mg/cycle in 5 mg/cycle increments. This corresponds to a 0 to 8.5% variation, on a mass of H<sub>2</sub>O to induced mass basis.

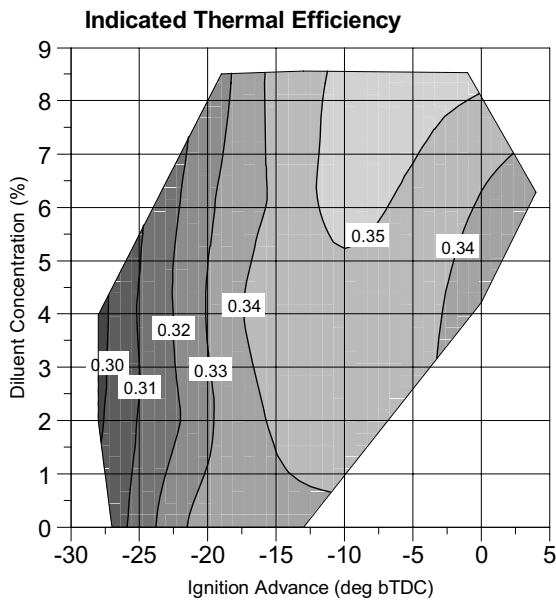


**Figure 33 Indicated thermal efficiency.**

At constant spark advance, the addition of water into the cylinder did not have a significant effect on the indicated thermal efficiency (Figure 33). The injected water allowed the ignition timing to be advanced through suppressing burn rate (Figure 34), which allowed MBT timing to be reached with and an increase in ITE.

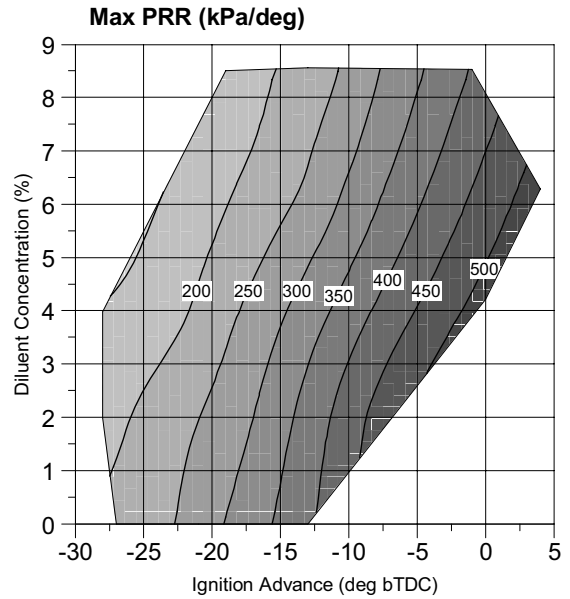


**Figure 34 Maximum pressure rise rate.**

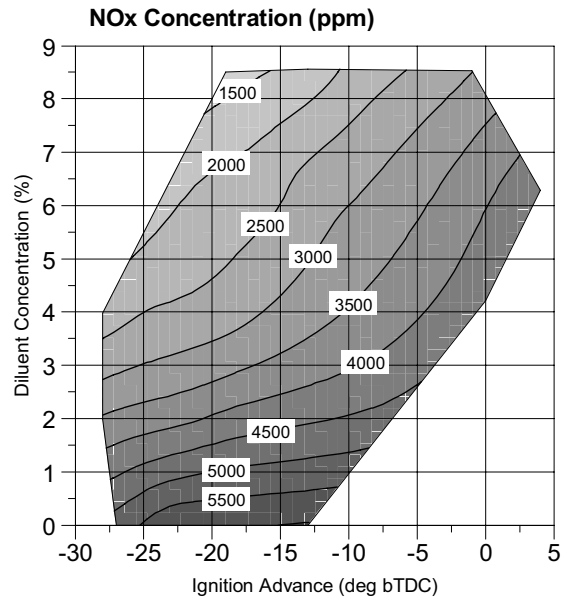


**Figure 35 NOx concentration.**

The addition of water at constant spark advance resulted in NOx concentration dropping from 6000 ppm to 1600 ppm (Figure 35) which may be attributed to reduced combustion temperatures. If the spark timing was advanced to the best indicated efficiency point for each case, NOx was only reduced to 2500 ppm.

The introduction of water into the cylinder had minimal effect on combustion stability (Figure 36). A slight increase of approximately 0.1% in COV was observed.

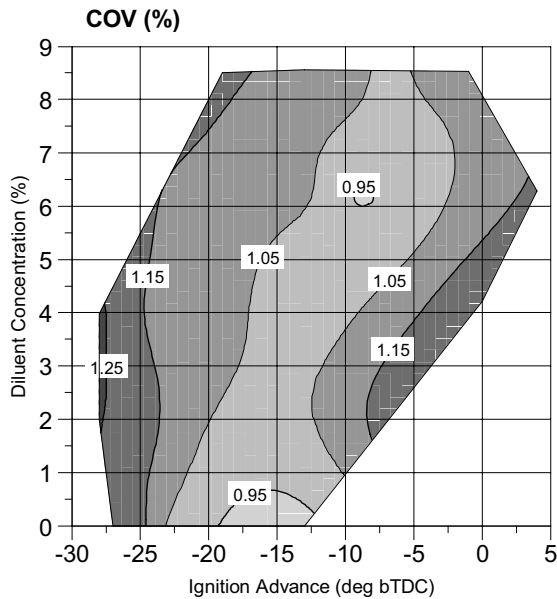


**Figure 36 Combustion stability.**

## DISCUSSION

### REVIEW OF RESULTS

Hydrogen fuelled IC engines have the potential to exceed current gasoline engine performance with lower NO<sub>x</sub> and near zero carbon and hydrocarbon emissions. Controlling NO<sub>x</sub> production, and combustion during high load operation, presents unique challenges for HICE's. The high combustion temperatures of near stoichiometric mixtures lead to high levels of NO<sub>x</sub>, and excessive combustion rates at higher load which in effect limit full load output.

The wide flammability limits of hydrogen permit high levels of dilution with air, exhaust gas or water before combustion stability deteriorates. Dilution is an effective strategy to lower NO<sub>x</sub> emissions and to moderate combustion rates.

NO<sub>x</sub> production has been shown to be more dependent on equivalence ratio than load. On boosted engines, high efficiency and low NO<sub>x</sub> can be achieved by running at  $\phi < 0.4$ . If a lean storage catalyst is used, NO<sub>x</sub> may be controlled and full load output can be increased by enriching mixtures up to the pre-ignition limit. In turbo charged engines, hydrogen fuel enables the control of load with mixture quality offering improvement to transient response.

External exhaust gas recirculation allows stoichiometric mixtures to be combusted without pre-ignition and reduces NO<sub>x</sub> emissions. The use of EGR at higher load is limited on a normally aspirated engine and may be problematic on a boosted engine. If required, a three-way catalyst can be used to further reduce NO<sub>x</sub> levels.

The concept of water injection has been demonstrated as an alternative to EGR that may extend full load

operation and reduce NO<sub>x</sub> emissions. A further reduction of NO<sub>x</sub> concentration may be realized if the amount of water injected is increased.

Water injection allows fast and accurate control of the dilution level. The amount of water injection is independent of fuel and air flow and may extend the full load output of naturally aspirated engines, where EGR cannot be used. Under boosted operation, water injection presents an alternative to supplying exhaust gas through the compressor at high load.

### TECHNOLOGY APPLICATION

A manifold injected hydrogen engine will return high thermal efficiency and low NO<sub>x</sub> emissions when operated lean of  $\phi = 0.5$ . Leaner operation also avoids backfire and pre-ignition. Resistance to back fire may be improved by using sequential port fuel injection with injection occurring late during the intake event. There will be a significant reduction in engine output due to intake air displacement and lean operation, and the reduced heat energy of the induced charge.

Power output may be increased further by engine up-sizing or boosting. If certain emissions regulations apply, operation maybe limited to lean mixtures to avoid excessive NO<sub>x</sub> production. Combusting richer mixtures will yield higher output but at the cost of increased engine NO<sub>x</sub> production. NO<sub>x</sub> aftertreatment may be applied in the form of SCR or an LNT at  $\phi < 1$ , unless  $\phi = 1$  operation can be sustained in which case a TWC may be deployed.

If higher specific output is required than that achieved when upsizing and boosting, then direct fuel injection can be used. Direct injection increases the calorific value of the mixture by a nominal 42% over manifold injection. The issue of backfire is avoided by delaying the injection event and operation at  $\phi = 1$  may be achieved if combustion rate is moderated and pre-ignition controlled.

Both EGR and water injection increase full load performance of hydrogen fuelled engines by allowing mixtures closer to stoichiometric to be combusted without abnormal combustion. These are alternatives for increasing specific power output if boosting or engine upsizing is not viable.

EGR and water injection also provide significant NO<sub>x</sub> reductions over normal unthrottled operation at similar loads. Either of these strategies could be employed to meet part load emissions constraints with or without engine boosting.

Full load NO<sub>x</sub> control is achievable with EGR or water injection without the power density losses of lean operation. Both of these strategies allow engines to operate with stoichiometric mixtures, facilitating the use of a three-way catalyst.

## CONCLUSION

- Dilution is required to increase specific power and control NOx
- Lean boosted operation returns high efficiency and low NOx emissions
- EGR extends higher load output over normal operation and reduces NOx.
- EGR permits stoichiometric combustion allowing the use of a TWC.
- Water injection is an effective alternative to EGR, with accuracy and response advantages.
- Water injection can be used in certain applications where EGR cannot or is undesirable.

## ACKNOWLEDGMENTS

The authors would like to thank the facilities staff and in particular Doug Barrett for their assistance throughout this project. Special thanks are due to David Caley and Walter O'Keefe for assistance given with water injection equipment.

## REFERENCES

1. Eichseder H., Wallner T., Freymann R. and Ringler J. The Potential of Hydrogen Internal Combustion Engines in a Future Mobility Scenario. SAE paper number 2003-01-2267, 2003
2. Kiesgen G., Kluting M., Bock C. and Fischer H. The New 12-Cylinder Hydrogen Engine in the 7 Series: The H2 ICE Age Has Begun. SAE paper number 2006-01-0431, 2006
3. Saanum I., Bysveen M., Tunestal P. and Johansson B. Lean Burn Versus Stoichiometric Operation with EGR and 3-Way Catalyst of an Engine Fuelled with Natural Gas and Hydrogen Enriched Natural Gas. SAE paper number 2007-01-0015, 2007
4. Wallner T., Ng H. and Peters R. The Effects of Blending Hydrogen with Methane on Engine Operation, Efficiency and Emissions. SAE paper number 2007-01-0474, 2007
5. Tang, X. et al. Ford P2000 Hydrogen Engine Dynamometer Development. SAE paper number 2002-01-0242, 2002
6. Rottengruber H. et al. Direct-Injection Hydrogen SI-Engine – Operation Strategy and Power Density Potentials. SAE paper number 2004-01-2927, 2004
7. Wimmer A., Wallner T., Ringler J. and Gerbig F. H2-Direct Injection – A Highly Promising Combustion Concept. SAE paper number 2005-01-0108, 2005
8. Verstraeten S., Sierens R. and Verhelst S. A High Speed Single Cylinder Hydrogen Fuelled Internal Combustion Engine. FISITA paper number F2004SC06
9. Stockhausen, W.F. et al. Ford P2000 Hydrogen Engine Design and Vehicle Development Program. SAE paper number 2002-01-0240, 2002

10. Berckmuller M. et al. Potentials of a Charged SI-Hydrogen Engine. SAE paper number 2003-01-3210, 2003
11. Swain M. and Adt R. Considerations in the Design of an Inexpensive Hydrogen-Fuelled Engine. SAE paper number 881630, 1988
12. Quader A.A. Why Intake Charge Dilution Decreases Nitric Oxide Emission from Spark Ignition Engines. SAE paper number 710009, 1971
13. Sierens R., Verhelst S. and Verstraeten S. EGR and Lean Combustion Strategies for a Single Cylinder Hydrogen Fuelled IC Engine. 10<sup>th</sup> EAEC European Automotive Congress, paper number EAEC05YU-EN15, 2005
14. Taxon M.N., Brueckner S.R. and Bohac S.V. Effect of Fuel Humidity on the Performance of a Single-Cylinder Research Engine Operating on Hydrogen. SAE paper number 2002-01-2685, 2002
15. Caley D. and Cathcart G. Development of a Natural Gas Spark Ignited Direct Injection Combustion System. NGV Global Conference, 2006
16. Cathcart G., Tubb J., Railton D. and Carlisle H. Application of Air-Assist Direct Fuel Injection to Pressure-Charged Gasoline Engines. SAE paper number 2002-01-0705, 2002
17. Heywood, J.B., "Internal Combustion Engine Fundamentals". McGraw-Hill Book Company, 1988. ISBN 0-07-100499-8

## CONTACT

Callan Bleechmore  
Orbital Corporation Ltd.  
Perth, Western Australia  
Tel: +61 8 9441 2409  
[cbleechmore@orbitalcorp.com.au](mailto:cbleechmore@orbitalcorp.com.au)

Simon Brewster  
Orbital Corporation Ltd.  
Perth, Western Australia  
Tel: +61 8 9441 2405  
[sbrewster@orbitalcorp.com.au](mailto:sbrewster@orbitalcorp.com.au)

## **ACRONYMS**

**aTDC<sub>f</sub>**: after Top Dead Centre Firing

**bTDC<sub>f</sub>**: before Top Dead Centre Firing

**CA**: Crank Angle

**CNG**: Compressed Natural Gas

**COV**: Coefficient of Variation

**DI**: Direct Injection

**EGR**: Exhaust Gas Recirculation

**EGT**: Exhaust Gas Temperature

**EVC**: Exhaust Valve Closing

**EVO**: Exhaust Valve Opening

**FPC**: Fuel per Cycle

**HICE**: Hydrogen fuelled Internal Combustion Engine

**ICE**: Internal Combustion Engine

**IMEP**: Indicated Mean Effective Pressure

**ISFC**: Indicated Specific Fuel Consumption

**ITE**: Indicated Thermal Efficiency

**IVC**: Intake Valve Closing

**IVO**: Intake Valve Opening

**LNT**: Lean NO<sub>x</sub> Trap

**MBT**: Maximum Brake Torque

**NO<sub>x</sub>**: Oxides of Nitrogen

**PFI**: Port Fuel Injection

**ppm**: Parts per Million

**PRR**: Pressure Rise Rate

**SCR**: Selective Catalytic Reduction

**SMD**: Sauter Mean Diameter

**SOI**: Start of Injection

**TWC**: Three Way Catalyst

**WPC**: Water per Cycle

**WOT**: Wide Open Throttle

**φ**: Equivalence Ratio